Ping *et al. BMC Genomics* (2025) 26:425
https://doi.org/10.1186/s12864-025-11616-8

BMC Genomics

RESEARCH Open Access

Whole-genome sequencing reveals patterns of runs of homozygosity underlying genetic diversity and selection in domestic rabbits

Xinxin Ping[1], Yuan Chen[1], Hui Wang[1], Zhuoya Jin[1], Qianting Duan[1], Zhanjun Ren[1] and Xianggui Dong[1*]

Abstract

Background Runs of homozygosity (ROH) are continuous segments of homozygous genotypes inherited from both parental lineages. These segments arise due to the transmission of identical haplotypes. The genome-wide patterns and hotspot regions of ROH provide valuable insights into genetic diversity, demographic history, and selection trends. In this study, we analyzed whole-genome resequencing data from 117 rabbits to identify ROH patterns and inbreeding level across eleven rabbit breeds, including seven Chinese indigenous breeds and four exotic breeds, and to uncover selective signatures based on ROH islands.

Results We detected a total of 31,429 ROHs across the autosomes of all breeds, with the number of ROHs (N_{ROH}) per breed ranging from 1316 to 7476. The mean sum of ROHs length (S_{ROH}) per individual was 493.84 Mb, covering approximately 22.79% of the rabbit autosomal genome. The majority of the detected ROHs ranged from 1 to 2 Mb in length, with an average ROH length (L_{ROH}) of 1.84 Mb. ROHs longer than 6 Mb constituted only 0.83% of the detected ROHs. The average inbreeding coefficient derived from ROHs (F_{ROH}) was 0.23, with F_{ROH} values ranging from 0.14 to 0.38 across breeds. Among Chinese indigenous breeds, the Jiuyishan rabbit exhibited the highest values of N_{ROH}, S_{ROH}, L_{ROH}, and F_{ROH}, whereas the Fujian Yellow rabbit had the lowest F_{ROH} values. In exotic rabbit breeds, the Japanese White rabbit displayed the highest values for N_{ROH}, S_{ROH}, L_{ROH}, and F_{ROH}, while the Flemish Giant rabbit had the lowest values for these metrics. Additionally, we identified 17 ROH islands in Chinese indigenous breeds and 22 ROH islands in exotic rabbit breeds, encompassing 124 and 186 genes, respectively. In Chinese indigenous breeds, we identified prominent genes associated with reproduction, including *CFAP206*, *RNF133*, *CPNE4*, *ASTE1*, and *ATP2C1*, as well as genes related to adaptation, namely *CADPS2*, *FEZF1*, and *EPHA7*. In contrast, the exotic breeds exhibited a prevalence of genes associated with fat deposition, such as *ELOVL3* and *NPM3*, as well as growth and body weight related genes, including *FAM184B*, *NSMCE2*, and *TWNK*.

Conclusions This study enhances our understanding of genetic diversity and selection pressures in domestic rabbits, offering valuable implications for breeding management and conservation strategies.

Keywords Rabbit, Runs of homozygosity, Inbreeding, Genome resequencing, ROH island

*Correspondence:
Xianggui Dong
xgdong@nwafu.edu.cn
[1]Key Laboratory of Animal Genetics, Breeding and Reproduction of Shaanxi Province, College of Animal Science and Technology, Northwest A&F University, Yangling 712100, China

Background

The domestic rabbit (*Oryctolagus cuniculus*), which originated in southern France approximately 1,400 years ago, is considered one of the recently domesticated species [1, 2]. Following initial colonization and trade, the rabbit has gradually dispersed worldwide [3, 4]. Currently, more than 400 distinct rabbit breeds are recognized globally [5]. Rabbits provide valuable resources for humans, including rabbit meat [6, 7], fur [8], and serve as valuable models for biomedical and basic research [9]. It is noteworthy that rabbits exhibit extreme phenotypic diversity, with different breeds showing considerable variation in weight, body structure, fur type, coat color, and ear length [10]. Additionally, there is considerable variation in litter size, growth rate, behavior, and commercial use among different rabbit breeds [11]. Therefore, research on rabbit genomic diversity represents a crucial genetic resource for understanding the genetic mechanisms underlying phenotypic variation, disease resistance, and environmental adaptation.

China, with its long history of rabbit domestication and breeding, plays a key role in the global rabbit industry. Chinese indigenous rabbits are integral to animal husbandry and are primarily distributed across provinces such as Sichuan, Shandong, Fujian, Hunan, and Jiangxi. These breeds are known for their adaptability to roughage, disease resistance, and high reproductive performance [12, 13]. However, constrained population sizes and intensive directional selection have resulted in elevated inbreeding levels in these rabbit populations. Such inbreeding increases population homozygosity, which adversely impacts several economically important traits and reduces genetic gain [14, 15].

Runs of homozygosity (ROH) are continuous stretches of homozygosity in the genome, resulting from the inheritance of identical haplotypes from both parents [16]. These segments can be detected through genotyping single nucleotide polymorphisms (SNPs) across the genome [17], reflecting the inbreeding level of animals [18, 19]. ROHs are primarily caused by population phenomena such as genetic drift, population bottlenecks, inbreeding, and strong directional selection [20]. ROHs provide valuable insights into population history and genetic diversity. ROHs arise from shared ancestors within a population; different population histories lead to distinct distributions of long ROHs and short ROHs. Specifically, short ROHs indicate more distant common ancestors and larger population sizes, whereas long ROHs reflect more recent common ancestors and smaller population sizes [21–23], as homozygous segments have not yet been broken down by recombination events. Over generations, early homozygous segments gradually become shorter due to meiotic recombination [22]. Changes in population size, influenced by breeding practices and genetic drift, affect the pattern of ROHs [24]. An increase in ROHs can lead to inbreeding depression and the emergence of deleterious recessive alleles [25, 26]. This elevated homozygosity exposes previously hidden harmful variants, leading to their rapid accumulation in the population [21, 22, 25]. Since natural selection cannot completely eliminate deleterious recessive alleles, their persistence can negatively impact reproductive performance, aging, and environmental adaptation in livestock [17]. Previous studies revealed that deleterious variants tend to cluster in ROH regions, especially long ROHs, linking to adverse traits in humans [25], pigs [27], cattle [28, 29] and chickens [30].

ROH evaluates the inbreeding degree by inbreeding coefficient (F_{ROH}), which is defined as the ratio of the total length of ROH (S_{ROH}) to the length of the autosomal genome of a species [31], being considered more effective for this purpose than pedigree data (F_{PED}) [31]. While F_{PED} estimates the proportion of identity by descent (IBD) in individual genome, it is limited in predicting distant relatives due to correlations through multiple lineages, often leading to an underestimation of inbreeding [32, 33]. With advancements of genomics, researchers have increasingly employed genome-wide polymorphism markers to predict individual homozygosity (F_{HOM}) [34]. However, this approach requires estimation of allele frequencies within the population [31]. Consequently, McQuillan [31] proposed using ROH to estimate individual inbreeding coefficients, referred to as F_{ROH}. F_{ROH} does not rely on pedigree information and provides a more accurate estimation of the self-mating across the genome, effectively detecting inbreeding resulting from common ancestors within up to 50 generations [35].

Strong directional selection increases the homozygosity of genomic regions, which leads to the occurrence of ROH. When a series of continuous SNPs are encompassed by ROHs and the proportion of ROH within the population surpasses a certain threshold, these regions are referred to as ROH islands (ROH hotspots), which are frequently used to identify selection signatures in livestock [36–38]. Mohamad et al. [36] found that among 12 fancy rabbit breeds and 4 meat rabbit breeds, the genes within ROH islands in meat rabbit breeds were more closely associated with traits such as body shape, body length, pigmentation processes, carcass traits, growth, and reproduction traits. In dairy cows, genes related to lactation and milk yield are predominantly located in ROH islands [39]. ROH islands may represent regions with low recombination or regions with a few harmful recessive alleles, thus maintaining the homozygosity of gene fragments. Positive selection is an important driving force for the formation of ROH islands, so it is very important to understand the potential genetic structure of animal genomes [23].

Recent studies have identified ROHs in cattle [40], pigs [41], sheep [42], rabbits [14, 36], and chickens [43], highlighting their significance for breeding management and resource conservation in livestock. However, limited knowledge exists regarding ROHs in the genomes of Chinese indigenous rabbit breeds. Therefore, based on genome-wide resequencing data from Chinese indigenous and exotic rabbit breeds, this study aims to characterize the whole-genome ROHs of rabbits, fully understand the ROH patterns and population history, and calculate several genomic inbreeding parameters. Subsequently, we evaluated the ROH islands in the genomes of indigenous and exotic breeds to identify distinct selection trends and candidate genes in different rabbit populations. These results provide valuable resources for understanding the genetic history and selection characteristics of rabbit populations and are crucial for preserving the diversity of rabbit genetic resources and guiding breeding management.

Methods

Sample collection, sequencing, and SNP calling

In this study, a total of 117 rabbits were analyzed, comprising seven Chinese indigenous rabbit breeds and four exotic rabbit breeds, which include three European breeds and one Japanese breed (Additional file 1: Table S1). Among the exotic rabbit breeds, genome sequencing data of New Zealand White rabbit and Japanese White rabbit were obtained from the NCBI SRA database under accession number SRP053211 [44]. Blood samples were collected from the marginal auricular vein of rabbits. Genomic DNA was extracted using the routine phenol-chloroform protocol. Briefly, blood samples were lysed with SDS and proteinase K at 56 °C for 2 h, followed by phenol-chloroform-isoamyl alcohol (25:24:1) extraction and ethanol precipitation. DNA pellets were washed with 70% ethanol, air-dried, and resuspended in TE buffer. The quality of DNA was measured using a NanoDrop 2000 (Thermo Scientific), and by 1% agarose gel electrophoresis. All samples showed A260/A280 ratios between 1.8 and 2.0 and high-molecular-weight bands without degradation. DNA yields ranged from 5 to 10 μg per sample, sufficient for downstream library construction and sequencing. Two paired-end libraries (150 bp) were constructed per sample following the manufacturer's protocol (Illumina), and sequencing was performed on the Illumina NovaSeq 6000 platform.

The raw data were filtered using fastp (v.0.23.4) [45] to remove low-quality bases and sequences. The filtering criteria included the removal of reads with more than 50% of bases having Phred quality scores less than 30. High-quality reads were aligned to the rabbit reference genome (UM_NZW_1.0) [46] using the BWA (v.0.7.17) tool [47]. Bam files were sorted using SAMtools (v.1.9) [48] and duplicate reads were deleted from individual sample alignments using Picard (v.2.25.5) [49]. The coverage depth ranged from 6.82× to 24.47×. Genomic variants for each sample were identified using the HaplotypeCaller module and the GVCF model with Genome Analysis Toolkit (GATK, v.4.4.0.0) software [50]. The GVCF files were merged and variants were filtered according to stringent criteria. The parameter was set as follows: "QD < 2.0 || FS > 60.0 || MQ < 40.0 || MQRankSum < -12.5 || ReadPosRankSum <-8.0". Additionally, SNPs with a genotype missing rate (--geno) > 0.01 and minor allele frequency (--MAF) < 0.05 were excluded from the population using PLINK (v.1.9) [51] for subsequent analysis.

Detection of runs of homozygosity

ROHs were identified in each sample using PLINK (v.1.9) on autosomes. The impact of linkage disequilibrium (LD) pruning on ROH detection varies significantly across populations, which potentially leads to underestimation of ROHs. Therefore, SNP data in this study were analyzed without LD pruning [52]. The following parameters were applied for ROH detection: (i) a minimal of 50 SNPs per ROH; (ii) a maximal gap of 1000 kb between the adjacent SNPs; (iii) a minimum SNP density of 1 SNP every 50 kb within each ROH (avoid the influence of homozygous fragments in SNP sparse region [53]); (iv) a minimum ROH length of 1000 kb (exclude relatively short fragments caused by linkage disequilibrium blocks [54]); (v) sliding windows of 50 SNPs across the genome; (vi) a maximum of 5 missing genotype; and (vii) a maximum of 3 heterozygous SNPs [22].

Based on segment length [36, 55], the identified ROHs were classified into four categories: $ROH_{(1–2\ Mb)}$ (ROH ≥ 1 Mb and < 2 Mb); $ROH_{(2–4\ Mb)}$ (ROH ≥ 2 Mb and < 4 Mb); $ROH_{(4–6\ Mb)}$ (ROH ≥ 4 Mb and < 6 Mb) and $ROH_{(6\ Mb)}$ (ROH ≥ 6 Mb). Additionally, these were grouped into three size-based categories: Small ($ROH_{(1–2\ Mb)}$), Medium ($ROH_{(2–4\ Mb)}$ and $ROH_{(4–6\ Mb)}$), and Large ($ROH_{(6\ Mb)}$). In addition, the number of ROHs (N_{ROH}), the mean sum length of ROHs (S_{ROH}) and the average length of ROHs (L_{ROH}) were calculated. The Pearson correlation coefficient (r) was used to assess the correlation between N_{ROH} and S_{ROH}.

Calculation of inbreeding coefficients and the effective population size

The genome inbreeding coefficients for each individual were obtained as the proportion of the autosomal genome covered by ROH, using the following equation [31]:

$$F_{\mathrm{ROH}} = \frac{L_{\mathrm{ROH}}}{L_{\mathrm{aut}}}$$

Where L_{ROH} is the total length of all ROHs in an individual's genome and L_{aut} is the total length of the 21 autosomes in the rabbit genome. In this study, the length of the rabbit autosomal genome was approximately 2,167,210 kb.

Additionally, the genomic inbreeding coefficient based on the observed and the expected number of the homozygous genotypes was calculated using PLINK (v.1.9) as follows [56]:

$$F_{HOM} = \frac{O_{HOM} - E_{HOM}}{L_{HOM} - E_{HOM}}$$

where E_{HOM} and O_{HOM} represent the expected and observed numbers of homozygous genotypes in the sample, respectively. L_{HOM} represent the total number of SNPs. The Pearson correlation coefficient (r) was calculated to assess the correlation between F_{ROH} and F_{HOM}.

The GONE software [57] was employed to estimate the recent effective population size (Ne) for each breed. GONE calculates LD between pairs of SNPs over a range of recombination rates and finds the series of Ne that best explains the observed LD spectrum. All simulations were run for 2,000 generations calculated in 400 bins. The linkage map of the rabbit autosomal genome reached a total length of 1,419 cM [58]. The average recombination rate for the map is approximately 0.52 cM/Mb, which was used as the parameter for Ne estimation. Each simulation was repeated 40 times with the default settings, to account for variance in Ne estimates across different runs.

Calculation of heterozygosity

Heterozygosity reflects the probability of a locus being heterozygous and serves as an indicator of population genetic diversity [59]. For each breed, we calculated both observed heterozygosity (Ho) and expected heterozygosity (He) using PLINK (v1.9).

Detection and gene annotation within ROH islands

ROH islands were identified by calculating the occurrence frequency of SNPs within ROH segments for each population. Specifically, SNP frequency was defined as the number of times a SNP appeared in all ROH divided by the total number of individuals in the respective population [60]. SNPs with a frequency of 70% or higher were considered candidate SNPs. Genomic regions containing contiguous candidate SNPs (inter-SNP distance < 1 Mb) exceeding this threshold were defined as ROH islands. Genes within these ROH islands were identified using bedtools (v.2.31.0) [61]. To investigate the biological function of these genes, we performed enrichment analysis through DAVID (v2024q2) [62], utilizing both the Kyoto Encyclopedia of Genes and Genomes (KEGG) and Gene Ontology (GO) databases. Functional categories with false discovery rate (FDR)-adjusted *P*-values < 0.05 were considered statistically significant.

Results

Distribution of runs of homozygosity

A total of 31,949,377 SNPs were identified through whole-genome resequencing of 117 rabbits across 11 breeds. After filtering, 15,372,621 SNPs remained in autosomal genomic regions. Using this SNP data, we identified a total of 31,429 ROHs (Additional file 1: Table S2). The number of ROHs (N_{ROH}) varied significantly among breeds, ranging from 1,316 in Flemish Giant rabbit to 7,476 in Jiuyishan rabbit (Fig. 1a). For each individual, the N_{ROH} ranges from 158 in Flemish Giant rabbit to 506 in Japanese white rabbit, with an average of 269 ROHs per individual (Fig. 1d). ROHs were predominantly located on OCU1-OCU3 (*Oryctolagus cuniculus* chromosome, OCU), OCU7, OCU12 and OCU14, with OCU7 having the highest count of 3,098, accounting for 9.86% of the total N_{ROH} (Fig. 1b). The mean sum of ROHs length (S_{ROH}) per individual was 493.84 Mb (Fig. 1e), with an average ROHs length (L_{ROH}) of 1.84 Mb (Fig. 1f), ranging from 1 Mb to 12.72 Mb. On average, ROHs covered 22.79% of the autosome genome. The longest ROH, spanning 12.72 Mb, was located on OCU3 in Sichuan White rabbit and contained 133,718 SNPs. A significant correlation ($P < 0.01$) was observed between N_{ROH} and S_{ROH} (Fig. 1c) with a correlation coefficient of 0.97 ($P = 1.77e\text{-}76$).

To better understand the distribution of ROH length across rabbit populations, we categorized ROH lengths into four groups: 1–2 Mb, 2–4 Mb, 4–6 Mb, and over 6 Mb (Fig. 1b and Additional file 1: Table S3). The distributions of ROHs across these length categories was not balanced. The majority of detected ROHs were shorter than 6 Mb, with the ROH $_{(1–2\ Mb)}$ category being the most prevalent, accounting for 72.36% of the total ROH number, while ROH $_{(6\ Mb)}$ comprised only 0.83%. When comparing different breeds, Jiuyishan rabbit showed a high proportion of homozygote segments in ROH $_{(1–2\ Mb)}$ and ROH $_{(2–4\ Mb)}$ categories. A similar trend was observed in Japanese white rabbit from the exotic breeds. These short ROH tracts likely indicate that the rabbit population has undergone more intense selective breeding in recent generations.

Genomic inbreeding parameters and the effective population size

To assess genomic breeding inferred from ROHs, we calculated the average inbreeding coefficient based on four different ROH length categories. As shown in Fig. 2a-b and Table S4 (Additional file 1), these values varied significantly among breeds and length categories. The

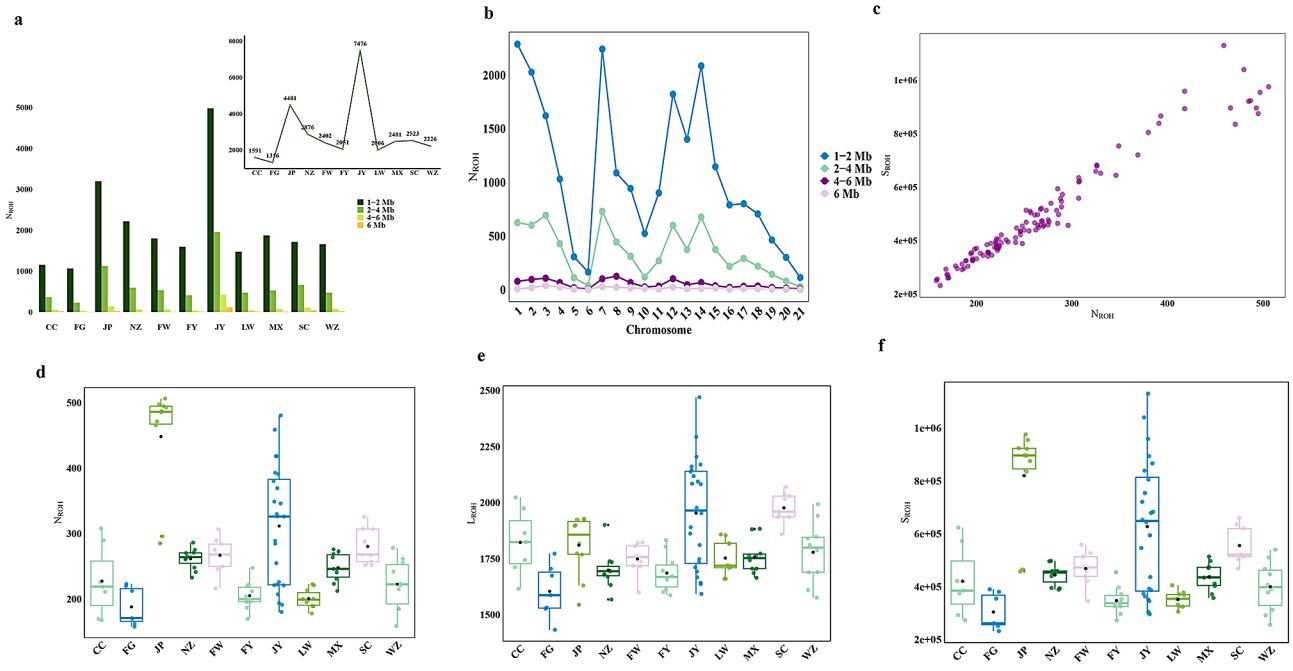

Fig. 1 Distribution patterns of genomic ROHs across different rabbit breeds. (**a**) Total number of ROHs and ROH categories by length in various rabbit breeds. (**b**) Distribution of ROH length categories across rabbit autosomes. (**c**) Correlation analysis between N_{ROH} and S_{ROH} in the rabbit population. (**d**-**f**) ROH-related metrics in various rabbit breeds: N_{ROH} represents the total number of ROHs. S_{ROH} represents the mean sum length of ROH, and L_{ROH} represents the average length of ROH

overall mean F_{ROH} across the rabbit population was 0.23. The Flemish Giant rabbit (0.14), Fujian Yellow rabbit (0.16), Laiwu Black rabbit (0.16) and Wanzai rabbit (0.18) exhibited lower average F_{ROH} values compared to other breeds (Fig. 2a, Additional file 1: Table S2). These findings were consistent with heterozygosity patterns (Additional file 1: Table S5), as these breeds also exhibited the higher average expected heterozygosity, indicating greater genetic diversity. In contrast, the Japanese White rabbit had the highest average F_{ROH} at 0.38 and the lower He (0.14), with the Jiuyishan rabbit also showing a relatively high average F_{ROH} of 0.28. Among the four ROH length categories, $F_{ROH\ (1–2\ Mb)}$ was higher than $F_{ROH\ (2–4\ Mb)}$, $F_{ROH\ (4–6\ Mb)}$ and $F_{ROH\ (6\ Mb)}$, with $F_{ROH\ (6\ Mb)}$ being notably lower than the other categories. The Japanese White rabbit had higher for $F_{ROH\ (1–2\ Mb)}$ and $F_{ROH\ (2–4\ Mb)}$ compared to other breeds, while the Jiuyishan rabbit had the highest values for $F_{ROH\ (4–6\ Mb)}$ and $F_{ROH\ (6\ Mb)}$. Conversely, Laiwu Black rabbit displayed low $F_{ROH\ (1–2\ Mb)}$, while $F_{ROH\ (2–4\ Mb)}$, $F_{ROH\ (4–6\ Mb)}$ and F_{ROH} for Fujian Yellow rabbit were lowest. The Flemish Giant rabbit exhibited very low inbreeding coefficients across all ROH length categories. The genomic SNPs heterozygosity based inbreeding coefficients (F_{HOM}) [55, 63] showed trends consistent with F_{ROH}, ranging from 0.14 to 0.58 (Fig. 2c).

Correlation analysis of the inbreeding coefficients revealed a significant positive correlation between F_{ROH} and F_{HOM} in most breeds ($P<0.05$) (Fig. 2e), with the highest correlation observed in Jiuyishan rabbit ($r=0.97$, $P=1.83e-15$). However, correlations were not significant in Laiwu Black rabbit, Japanese White rabbit and New Zealand White rabbit ($P>0.05$). We also analyzed the correlation among F_{ROH}, F_{HOM} and inbreeding coefficient based on different ROH length categories for the entire population (Fig. 2d). Our results indicated high correlations among all inbreeding coefficient ($P<0.05$). Specifically, $F_{ROH\ (1–2\ Mb)}$ and $F_{ROH\ (2–4\ Mb)}$ were most strongly correlated with overall F_{ROH}, suggesting a potential effect of ancestral inbreeding in the rabbit population. F_{HOM} was significantly correlated with F_{ROH} ($r=0.89$, $P=1.21e-41$). These findings demonstrate that ROH provides a reliable measure of inbreeding levels and can be effectively utilized in breeding programs, even in the absence of pedigree records.

Furthermore, estimates of Ne are important to predict the impacts of inbreeding on the evolutionary dynamics of populations. Ne is described as an idealized Wright Fisher population, which is supposed to produce the same genetic parameter values as the studied population, such as the rate of influence by genetic drift [64]. Thus, we assessed Ne of each rabbit breed over a range of 200 to 4 generations. The results indicated significant variation in Ne among the breeds (Fig. 2f-g). Most breeds displayed a consistent trend in Ne. Specifically, for the Wanzai rabbit, Ne gradually decreased up to 100 generations ago, then increased from 100 to 40 generations ago,

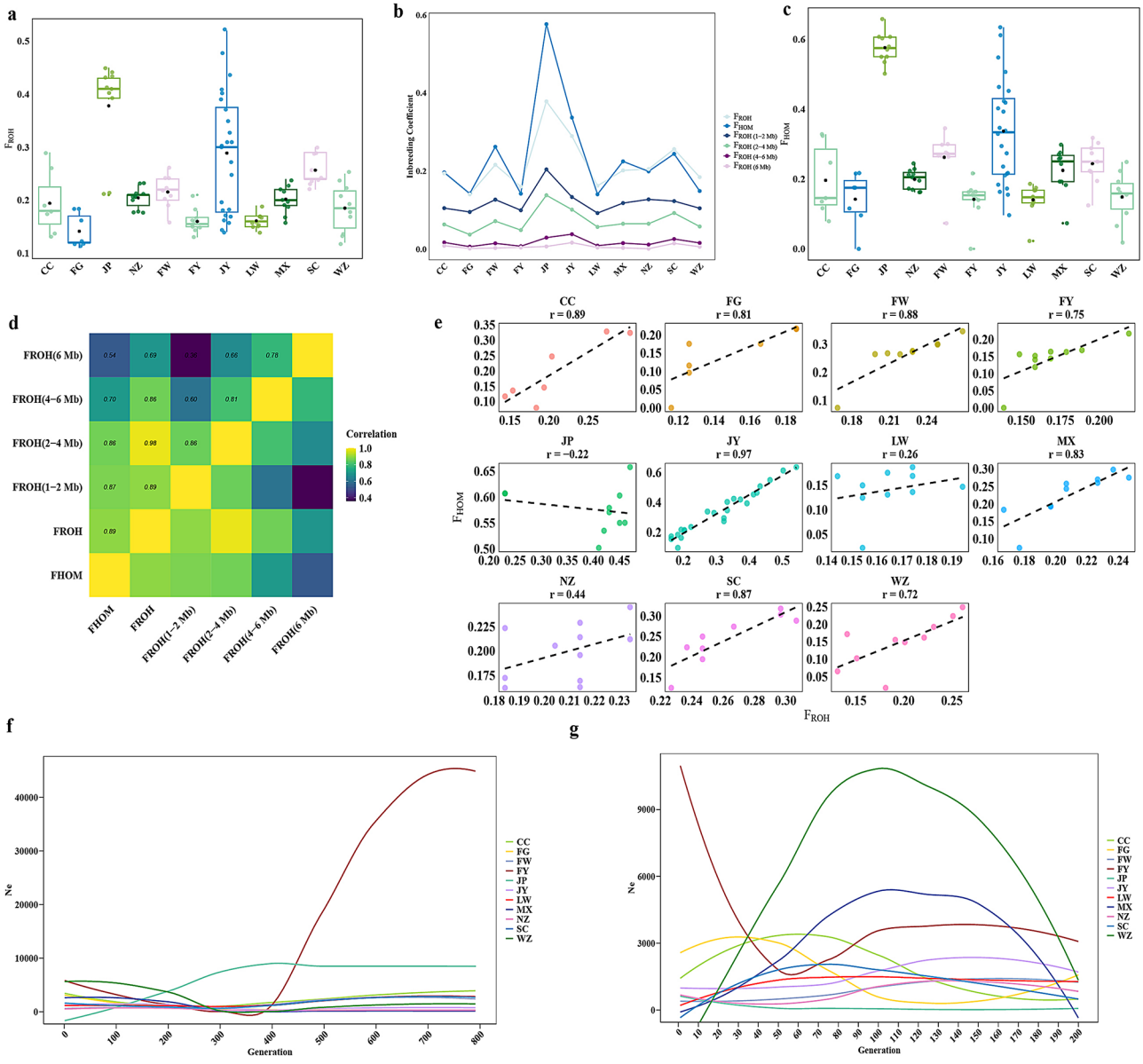

Fig. 2 Inbreeding coefficient and effective population size. (**a**) Inbreeding coefficient based on ROHs (F_{ROH}). (**b**) Comparison of inbreeding coefficient based on different metrics across various rabbit breeds. (**c**) Inbreeding Coefficient based on SNP heterozygosity (F_{HOM}). (**d**) Correlation between different inbreeding coefficients. (**e**) Correlation of F_{ROH} and F_{HOM} in each breed. (**f**-**g**) Effective population size over generations

followed by a sharp decline in 55 generations. The Fujian Yellow rabbit had the highest estimated Ne in 500 generations ago, however, showed a sharp decline in 550 to 460 generations ago and the Ne had a violent increase in recent 25 generations. The Japanese White rabbit had the smallest estimated Ne during the period from 200 to 20 generations ago and a relatively stable trend in 230 generations ago.

ROH island and functional analysis of related genes

Under strong selection pressure, beneficial mutations are likely to become fixed within particular genomic regions, leading to the formation of ROH islands in these areas [23]. To determine the genomic regions with the high proportion of homozygosity that potentially harbor targets of positive selection, we identified a total of 17 ROH islands in Chinese indigenous breeds, encompassing 78,586 high frequency SNPs (Table 1; Fig. 3a). These islands were distributed on seven autosomes, ranging from 0.25 Mb to 3.53 Mb in length, with an average length of 1.30 Mb. More detailed statistics on the detected ROH islands are provided in Tables 1 and 2. The longest ROH island was located on OCU9, spanning from 8,390,863 bp to 11,922,134 bp and containing 12,840 SNPs. On OCU7, we identified five ROH islands that covered 4.07% of OCU7 and included the

Table 1 The characteristics of ROH islands and associated genes in Chinese indigenous rabbits

Rank	OCU	Genomic regions			Number of SNPs	Genes
		Start	End	Length (Mb)		
ROH1	3	141,237,001	141,769,638	0.53	126	-
ROH2	4	76,507,734	77,625,454	1.12	4234	-
ROH3	7	63,408,689	64,383,426	0.97	2903	-
ROH4	7	66,723,305	68,437,480	1.71	3085	-
ROH5	7	107,281,595	108,265,090	0.98	4011	-
ROH6	7	135,257,048	137,629,393	2.37	8130	-
ROH7	7	150,943,607	151,955,186	1.01	2352	*FEZF1, CADPS2, RNF133*
ROH8	8	45,558,497	48,747,450	3.19	13,367	-
ROH9	9	8,390,863	11,922,134	3.53	12,840	-
ROH10	12	70,810,160	71,102,152	0.29	845	-
ROH11	12	74,739,976	75,416,148	0.68	1321	*EPHA7*
ROH12	12	81,594,775	81,845,338	0.25	660	*CFAP206*
ROH13	12	82,984,821	83,660,807	0.68	1998	-
ROH14	14	478,999	1,838,529	1.36	5816	*ASTE1, ATP2C1, CPNE4*
ROH15	14	3,554,868	4,689,549	1.13	4205	-
ROH16	14	32,242,887	33,156,219	0.91	3817	-
ROH17	15	61,089,079	62,448,485	1.36	8876	-

OCU: Oryctolagus cuniculus chromosome

genes *CADPS2*, *FEZF1* and *RNF133*. Within the 17 ROH islands, we identified 124 genes in Chinese indigenous breeds. These include genes associated with economic traits, particularly reproductive performance such as *CFAP206*, *RNF133*, *CPNE4*, *ASTE1*, and *ATP2C1* [65–69], as well as involved in feeding behavior, olfactory system development and thermo-tolerance including *CADPS2*, *FEZF1*, and *EPHA7* [70–72], which contribute to the adaptation and survival of Chinese indigenous rabbits in various environments.

We also detected 22 ROH islands covering 75,655 SNPs in exotic rabbit breeds (Table 2; Fig. 3b). The longest ROH island, spanning 4.23 Mb, was located on OCU7 and contained 8,144 SNPs, while the shortest, at only 2.21 kb, was found on OCU14 and contained just 24 SNPs. Notably, there are 5 ROH islands on OCU14, with the longest spanning 1.42 Mb. In exotic rabbit breeds, we identified 186 genes within 22 ROH islands, many of which are associated with fat deposition and growth traits such as *FAM184B*, *ELOVL3*, *NPM3*, and *TWNK* [73–85]. These genes are crucial for meat production, skeletal development and body weight in various livestock species.

Gene enrichment analysis of ROH island candidate genes revealed significant functional divergence between Chinese indigenous and exotic rabbit breeds (Fig. 4). Chinese indigenous breeds showed prominent enrichment for neuronal functions (Fig. 4a), particularly membrane depolarization during action potential (GO:0086010) and voltage-gated sodium channel activity (GO:0005248). These breeds also exhibited enrichment in cell adhesion processes (GO:0007156, GO:0044331) and immune-related pathways including B cell receptor signaling (GO:0050853). These results suggest strong selection pressure in Chinese indigenous breeds favoring neurological development and immune competence, which may underlie their enhanced stress tolerance. Conversely, exotic breeds demonstrated greater enrichment for metabolic pathways (Fig. 4b), featuring protein ubiquitination (GO:0016567), visual perception (GO:0007601), and the Hedgehog signaling pathway (ocu04340). This enrichment pattern reflects distinct selection priorities in exotic breeds, with apparent emphasis on metabolic efficiency and growth regulation, contrasting sharply with the adaptation-driven selection observed in Chinese indigenous populations.

Discussion

Domestication, selection, and crossbreeding have significantly shaped the genomes of domestic animals, resulting in a diverse array of breeds and populations within species [86]. These genetic resources have been utilized to explore the genetic mechanisms underlying extreme morphological and physiological traits [38]. The Chinese indigenous rabbit, as a unique and relatively underexplored resource, offers valuable insights into the genetic structure of phenotypic traits and serves as a model for understanding the genetic basis of these traits in other mammals. In this study, we analyzed patterns of ROHs and genomic inbreeding level in both Chinese indigenous and exotic rabbits. Our results confirmed that ROHs are frequent and widespread throughout the rabbit genome. The measure of F_{ROH} proved to be as an effective method for estimating inbreeding levels in populations, while

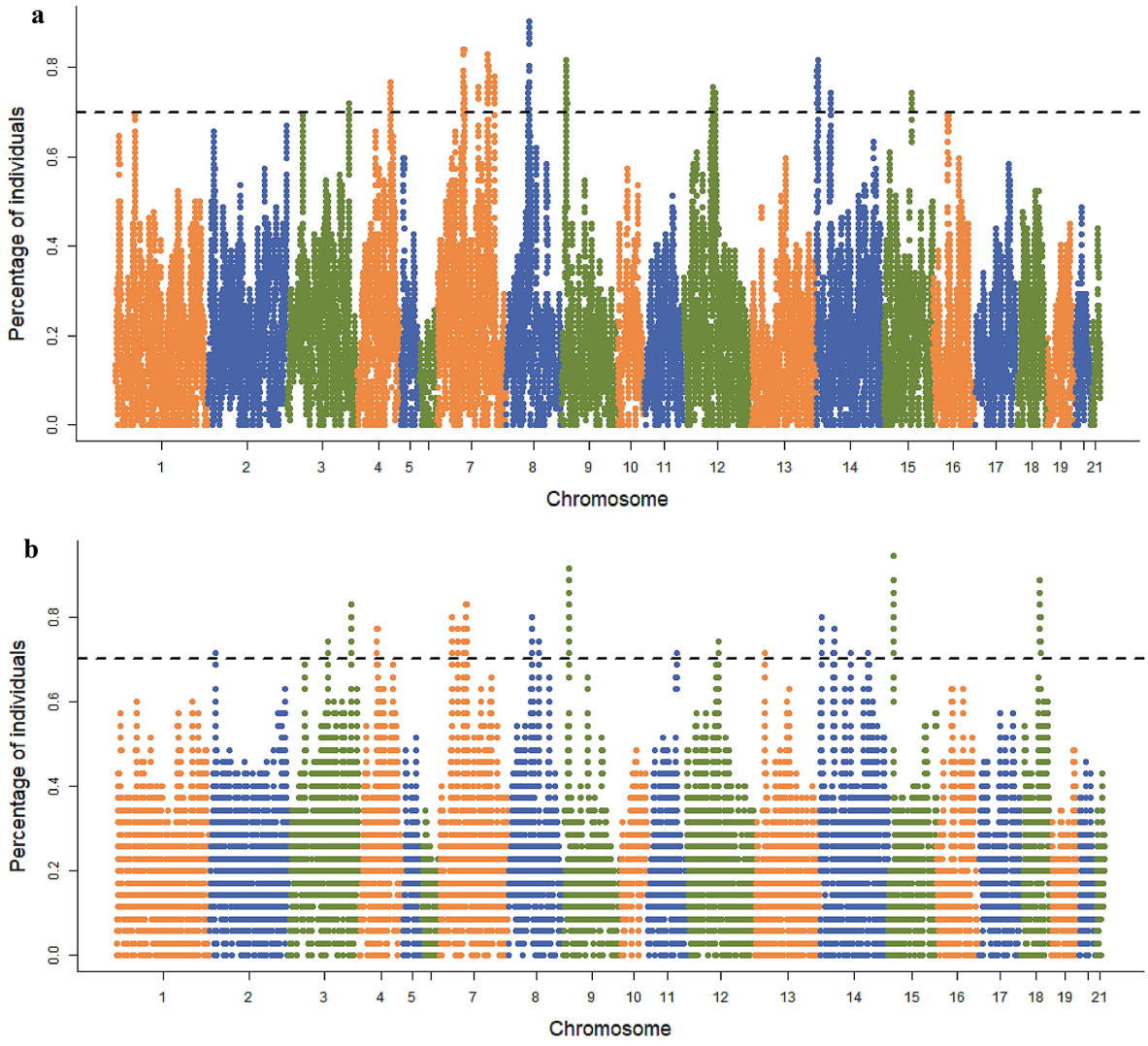

Fig. 3 Distribution of ROH islands in different rabbit populations. (**a**-**b**) Manhattan plots illustrating the percentage occurrence of each SNP within ROH regions for Chinese indigenous rabbits (**a**) and exotic rabbits (**b**)

ROH islands reflect genomic variations resulting from changes in population size and selection pressures.

Overall, the number and length of ROHs vary among breeds, likely attributed to breed-specific factors. Our results indicated that the average number of ROHs per individual was 269, which is greater than that reported for cattle, sheep, red deer and chickens [29, 43, 87, 88]. This suggests that domestic rabbits may have experienced frequent inbreeding or substantial selection pressure. Our findings align with a previous report of elevated ROH counts in meat rabbit populations [36], with the breeds in our study demonstrating similarly high N_{ROH} values. This increased homozygosity likely reflects the cumulative effects of intensive artificial selection for production traits in meat rabbit breeding programs [36]. The majority of ROHs were short (1–2 Mb), comprising 72.36% of detected ROH and covering 12.34% of the rabbit autosomal genome. Selection can fix loci associated with phenotypic traits, leading to the creation of homozygous segments due to non-random linkage of adjacent loci [89]. Long ROH fragments are more susceptible to recombination and disruption by random genetic processes, which can fragment them into shorter segments, thereby increasing number of short ROHs [23], Consequently, short ROHs can reflect the population structure of ancestors. Our findings revealed that the short ROHs were prevalent throughout the rabbit genome, indicating the rabbit population has undergone ancestral inbreeding. Additionally, the Japanese White rabbit and New Zealand White rabbit exhibited a higher average number of short ROHs compared to most Chinese indigenous breeds, likely due to more intense artificial selection during breeding. This selection has fixed

Table 2 The characteristics of ROH islands and associated genes in exotic rabbits

Rank	OCU	Genomic regions			Number of SNPs	Genes
		Start	End	Length (Mb)		
ROH1	2	8,840,090	8,881,116	0.04	180	*FAM184B*
ROH2	3	82,179,391	82,199,540	0.02	25	-
ROH3	3	140,447,253	141,826,110	1.38	1981	*NSMCE2*
ROH4	4	31,456,496	32,507,805	1.05	7541	-
ROH5	7	24,675,488	25,103,929	0.43	2872	-
ROH6	7	39,624,486	40,231,707	0.61	1867	-
ROH7	7	56,421,480	57,077,571	0.66	2356	-
ROH8	7	63,505,666	67,740,551	4.23	8144	-
ROH9	8	46,826,773	47,204,185	0.38	1370	-
ROH10	8	48,340,572	48,745,613	0.41	1505	-
ROH11	8	67,985,906	68,470,576	0.48	949	-
ROH12	9	7,989,219	9,741,915	1.75	4927	-
ROH13	11	70,150,147	70,275,731	0.13	363	-
ROH14	12	83,000,162	83,983,589	0.98	3118	-
ROH15	13	21,061,423	21,489,607	0.43	1249	-
ROH16	14	3,709,445	5,129,888	1.42	6317	-
ROH17	14	30,151,468	30,310,308	0.16	631	-
ROH18	14	32,241,869	33,403,998	1.16	6204	*TWNK, NPM3*
ROH19	14	68,580,709	68,582,917	0.00	24	-
ROH20	14	117,462,349	117,563,695	0.10	813	-
ROH21	15	9,414,642	11,573,951	2.16	13,050	-
ROH22	18	45,533,236	47,511,044	1.98	10,169	*ELOVL3*

OCU: Oryctolagus cuniculus chromosome

more loci associated with economic traits and resulted in the formation of additional homozygous segments.

Among the exotic rabbit breeds, the Japanese White rabbit had the highest average N_{ROH} at 448, compared to other breeds. In contrast, the Flemish Giant rabbit had a lower average N_{ROH} of 188. Similarly, the Japanese White rabbit exhibited the highest mean of S_{ROH} at 819.96 Mb, while the Flemish Giant rabbit had a lower mean S_{ROH} of 304.17 Mb. These results indicate a frequent occurrence of ROH in the Japanese White rabbit, suggesting that this breed has undergone a significant bottleneck period, leading to a decrease in Ne [87, 90]. The Ne analysis revealed that the Japanese White rabbit had the smallest population size 200 generations ago. As an important experimental rabbit breed in China, the Japanese White rabbit may be maintained in a relatively closed environment, which can increase inbreeding process and reduce genetic diversity, thereby affecting the level of homozygosity.

The inbreeding coefficients, calculated based on ROH segments, ranged from 0.14 to 0.38, with an average F_{ROH} of 0.23. This illustrates that rabbit populations exhibit significant inbreeding and lower genetic diversity. Compared to other breeds, Japanese White rabbit had the highest F_{ROH}, consistent with their increased homozygosity and higher inbreeding levels. Contrasty, Flemish Giant and Fujian Yellow rabbits showed lower inbreeding coefficients and higher heterozygosity, suggesting these breeds have experienced relatively limited inbreeding and maintained greater genetic diversity. This pattern may result from the intentional introduction of genetic material from other rabbit breeds during their breeding history. Additionally, we calculated the correlation coefficients between four different ROH length categories and total F_{ROH}. A strong correlation was found between $F_{ROH\ (1–2\ Mb)}$ and F_{ROH}, supporting the hypothesis that short ROHs are indicative of more distant inbreeding events. This correlation provides a useful methodological approach for assessing inbreeding levels and mitigating inbreeding depression in rabbit breeding programs. Furthermore, we observed a strong overall correlation between F_{ROH} and F_{HOM}, consistent with findings previously reported in rabbits [36], pigs [41], sheep [42], cattle [55] and chickens [43]. This consistency across multiple species confirms that F_{ROH} serves as a reliable indicator for estimating population inbreeding levels. However, Japanese White rabbit exhibited a negative correlation, which may be attributed to F_{HOM} including all homozygous genotypes in its calculations, encompassing both single-locus homozygous genotypes and extended homozygous regions. This inclusion could increase random error and obscure various historical events such as inbreeding, selection, and recombination.

The Ne results indicated a steady trend across most breeds 250 generations ago. Approximately 550 to 300 generations ago, Ne declined for most breeds. The

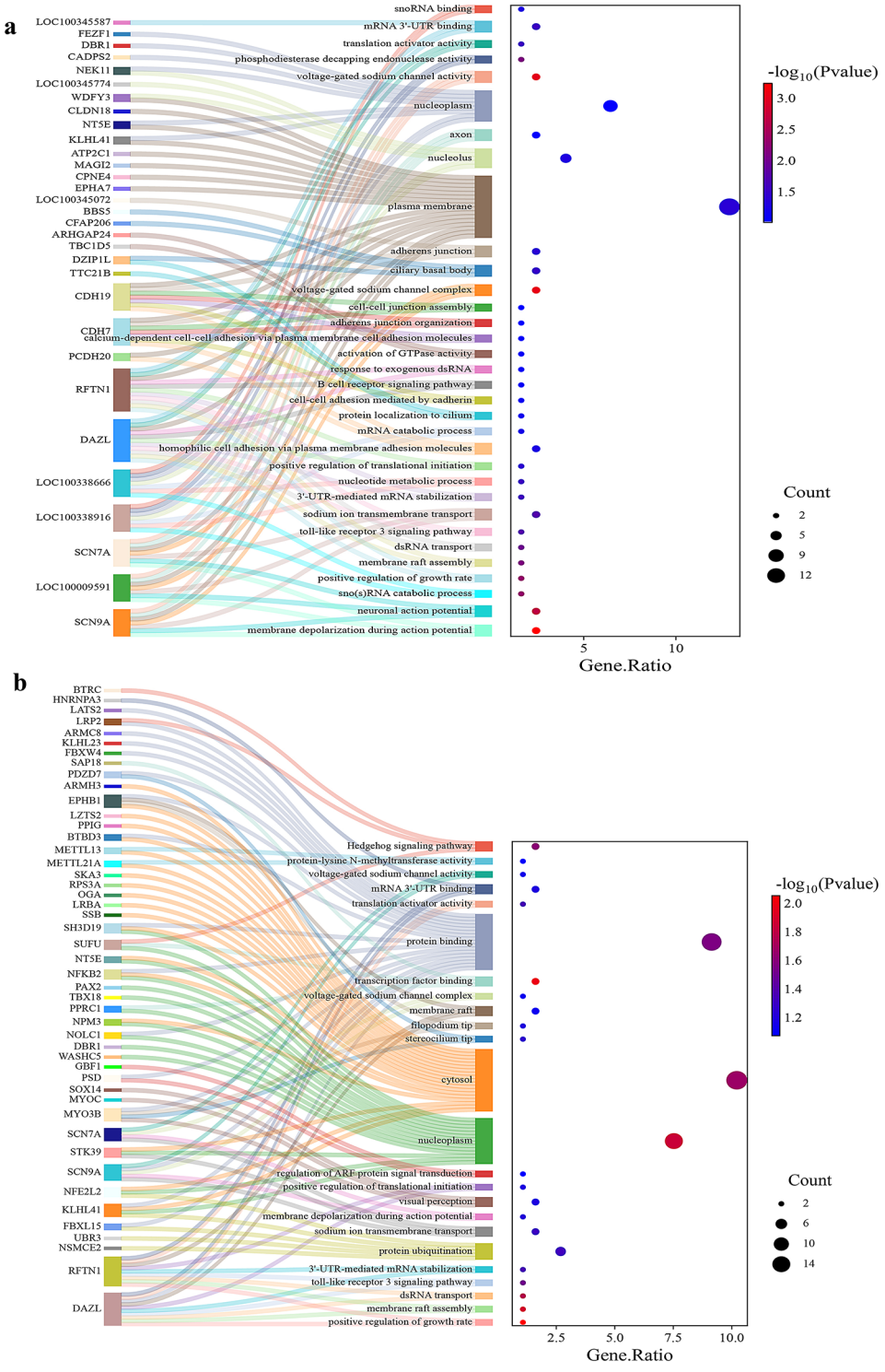

Fig. 4 Gene enrichment analysis within ROH islands in Chinese indigenous and exotic rabbits. (**a**-**b**) Gene ontology (GO) and Kyoto Encyclopedia of Genes and Genomes (KEGG) analysis of genes derived from ROH islands for Chinese indigenous rabbits (**a**) and exotic rabbits (**b**)

Wanzai rabbit exhibited a sharp decline, showing a steeper downward trend. This decline is likely due to artificial selection, which may have reduced genetic diversity. F_{ROH} can trace historical inbreeding events back to around 50 generations [91]. Notably, the Ne of the Japanese White rabbit was lowest between 50 and 18 generations, aligning with the highest values for $F_{ROH\ (1–2\ Mb)}$ and $F_{ROH\ (2–4\ Mb)}$. However, the Jiuyishan rabbit exhibited

higher values for $F_{ROH\ (4–6\ Mb)}$ and $F_{ROH\ (6\ Mb)}$ compared to other breeds. This finding was not accompanied by a lower Ne, which may be due to limitations in the software and methods used for estimating Ne. The estimation of Ne can be significantly influenced by the method applied, and values based on linkage disequilibrium might be underestimated due to the physical linkage between SNPs [92, 93].

Understanding the genetic mechanisms underlying crucial economic traits is indispensable in rabbit breeding. In our analysis of indigenous versus exotic rabbit breeds, we aimed to identify genomic regions under selective pressure by examining ROH islands. In Chinese indigenous rabbit breeds, we identified four crucial genes (*CFAP206*, *RNF133*, *CPNE4*, and *ATP2C1*) associated with reproductive traits, including sperm motility [67, 69], oocyte maturation [94, 95], and gestational nutrient allocation [66, 96]. *CFAP206* (Cilia and flagella associated protein 206), located within an ROH island on OCU12, plays an essential role in sperm flagellar integrity, with previous studies in mice [67] and pigs [97] demonstrating its direct impact on fertility. The *RNF133* gene encodes a testis-specific E3 ubiquitin-protein ligase that is critically important for proper sperm function during spermiogenesis, where its deficiency leads to significant fertility impairments [69]. Previous research has established that *CPNE4* gene regulates muscle glycogen and glucose metabolism during pregnancy in both cattle and sheep, identifying it as a prominent fertility-related candidate gene [66, 96]. *ATP2C1* gene shows specific expression patterns mediating communication between oocytes and surrounding cumulus cells during blastocyst formation in mice [68], indicating its crucial role in oocyte maturation and developmental competence [94, 95]. These ROH island genes collectively reveal the strong selection pressure exerted on reproductive traits during the directional breeding of Chinese indigenous rabbits. The long-term selection for individuals with superior reproductive performance has driven the fixation of favorable alleles at these loci, resulting in their increased homozygosity through generations of selective breeding. Our analysis also revealed several adaptation-related genes within ROH islands of Chinese indigenous rabbit breeds, including *CADPS2*, *FEZF1* and *EPHA7*, which collectively reflect their environmental adaptation processes. The *CADPS2* gene, encoding a calcium-dependent secretion activator that regulates neuronal exocytosis, has been associated with dietary behavior in pigs [70]. This suggests its potential involvement in the genetic adaptation of food selection behaviors under extensive farming conditions. *FEZF1* plays an essential role in olfactory system and sensory neuron development [71], and its selective retention may enhance foraging efficiency and predator avoidance capabilities in complex natural environments. *PHA7* has been demonstrated to contribute to tropical climate adaptation in chickens [72].

Analysis of ROH islands in exotic rabbit breeds identified five key candidate genes (*ELOVL3*, *NPM3*, *FAM184B*, *TWNK*, and *NSMCE2*) predominantly associated with lipid deposition, growth regulation, and body weight determination. The enrichment patterns of these genes clearly reflect the strong directional selection pressure exerted on exotic breeds under intensive breeding systems. As a member of fatty acid elongate family [77], the *ELOVL3* gene has been proved to significantly affect back fat thickness and intramuscular fat deposition in pigs [78, 79] and chickens [80]. *NPM3* may participate in the energy metabolism mode of exotic breeds to adapt to the high-energy feed environment by regulating the browning process of adipose tissue [81]. *FAM184B*, as a pleiotropic gene, is associated with body weight [73, 74], meat quality [75] and bone development [85]. The *TWNK* and *NSMCE2* genes are closely related to the growth and development of chickens [84] and human dwarfism [98]. These candidate genes collectively elucidate the distinctive genomic signatures of exotic rabbit breeds that have emerged through intensive artificial selection targeting growth performance, meat quality traits, and standardized body conformation.

Domestic rabbits exhibit substantial genetic diversity, providing valuable insights into the genetic structure underlying phenotypic variations. ROH can be employed to shed light on the population history of rabbits and reveal the selection signatures across different breeds. Understanding genomic changes during rabbit domestication and identifying genes underlying economic traits are crucial for enhancing breeding practices. These genetic insights can also advance breeding strategies and improving overall breeding outcomes [1, 99].

Conclusions

This study examined the patterns of ROH and estimated inbreeding coefficients based on ROH in 11 rabbit breeds using whole-genome resequencing data. In summary, ROH are frequent and ubiquitous, with short ROHs predominating in the rabbit genome, while long ROHs are relatively rare, suggesting that ancient inbreeding has influenced rabbit population. The F_{ROH} across the rabbit population was relatively high. The strong correlation between F_{ROH} and F_{HOM} indicates that F_{ROH} is an effective metric for quantifying inbreeding level and assessing genetic relationship within rabbit population. We detected a total of 17 ROH islands in Chinese indigenous breeds and 22 ROH islands in exotic rabbit breeds. We identified some genes related to reproduction (*CFAP206*, *RNF133*, *CPNE4*, and *ATP2C1*) and adaptation (*CADPS2*, *FEZF1* and *EPHA7*) in Chinese indigenous breeds, and some genes related to fat deposition, growth and weight

(*ELOVL3*, *NPM3*, *FAM184B*, *TWNK*, and *NSMCE2*) in exotic breeds. These findings provide valuable insights for the directional selection pressure experienced by rabbits. Overall, ROH analyses can inform practical breeding programs by optimizing selection schemes, minimizing inbreeding depression, enhancing the improvement of desirable traits, and supporting the sustainable utilization of rabbit genetic resources.

Abbreviations

E_{HOM}	The expected numbers of homozygous genotypes
F_{HOM}	The average inbreeding coefficient derived from SNP homozygosity
F_{PED}	The average inbreeding coefficient derived from pedigree data
F_{ROH}	The average inbreeding coefficient derived from ROHs
GO	Gene Ontology
IBD	Identity by descent
KEGG	The Kyoto Encyclopedia of Genes and Genomes
L_{aut}	The total length of the rabbit autosomes genome
LD	Linkage disequilibrium
L_{HOM}	The total number of SNPs
L_{ROH}	The average ROHs length
MAF	Minor allele frequency
Ne	Effective population size
N_{ROH}	The number of ROHs
OCU	Oryctolagus cuniculus chromosome
O_{HOM}	The observed numbers of homozygous genotypes
ROHs	Runs of homozygosity
SNPs	Single nucleotide polymorphisms
S_{ROH}	The mean sum of ROHs length

Supplementary Information

The online version contains supplementary material available at https://doi.org/10.1186/s12864-025-11616-8.

Supplementary Material 1

Acknowledgements

We are grateful to Researcher Xiping Xie from the Fujian Academy of Agricultural Sciences, Zhibiao Xiao from the Ningyuan Animal Husbandry and Aquatic Affairs Center of Hunan Province, Yongzhong Ye, Director of the Wanzai Rabbit Breeding Farm in Jiangxi Province, and Yongwei Zhi from Inner Mongolia Dongda Biotechnology Co., Ltd., for their assistance in sample collection. We thank the High-Performance Computing Center of NWAFU for providing computing resources.

Author contributions

XD conceived and designed the project. XP performed the experiments and analyzed the data. XP, YC handled the visualization. HW, ZJ and QD collected samples. ZR recruited animal resources. XP and XD wrote and revised the manuscript. All authors read and approved the final draft.

Funding

This work was supported by the Chinese Universities Scientific Fund (no. 2452020187).

Data availability

All raw genome sequencing data generated during the current study have been deposited in the National Center for Biotechnology Information (NCBI) Sequence Read Archive (SRA) database with the BioProject accession numbers PRJNA1224525 and PRJNA1198406.

Declarations

Ethical approval

All experimental protocols involving animals were approved by the Institutional Animal Care and Use Committee (IACUC) of Northwest A&F University (Approval No. 202205A29). This study strictly adhered to the Guidelines for the Ethical Review of Laboratory Animal Welfare (GB/T 35892 – 2018) established by the Welfare and Ethics Committee of the Chinese Association for Laboratory Animal Sciences (CALAS). All procedures were designed to minimize animal discomfort, with blood collection exclusively performed via non-terminal marginal ear vein puncture without anesthesia.

Consent for publication

Not applicable.

Competing interests

The authors declare no competing interests.

Received: 11 February 2025 / Accepted: 21 April 2025
Published online: 29 April 2025

References

1. Carneiro M, Rubin C-J, Di Palma F, Albert FW, Alföldi J, Barrio AM, et al. Rabbit genome analysis reveals a polygenic basis for phenotypic change during domestication. Science. 2014;345:1074–9.
2. Clutton-Brock J. A natural history of domesticated mammals. Praehistorische Z. 1990;65:73–6.
3. Queney G, Ferrand N, Weiss S, Mougel F, Monnerot M. Stationary distributions of microsatellite loci between divergent population groups of the European rabbit (Oryctolagus cuniculus). Mol Biol Evol. 2001;18:2169–78.
4. Flux J, Fullagar P. World distribution of the rabbit (Oryctolagus cuniculus). Acta Zoologica Fennica.; 1983.
5. Scherf B, Pilling D. The second report on the state of the world's animal genetic resources for food and agriculture. Rome: Commission on Genetic Resources for Food and Agriculture assessments; 2015.
6. Dalle Zotte A, Szendrő Z. The role of rabbit meat as functional food. Meat Sci. 2011;88:319–31.
7. Cullere M, Dalle Zotte A. Rabbit meat production and consumption: state of knowledge and future perspectives. Meat Sci. 2018;143:137–46.
8. Dorożyńska K, Maj D. Rabbits– their domestication and molecular genetics of hair coat development and quality. Anim Genet. 2021;52:10–20.
9. Mage RG, Esteves PJ, Rader C. Rabbit models of human diseases for diagnostics and therapeutics development. Dev Comp Immunol. 2019;92:99–104.
10. Carneiro M, Afonso S, Geraldes A, Garreau H, Bolet G, Boucher S, et al. The genetic structure of domestic rabbits. Mol Biol Evol. 2011;28:1801–16.
11. Lebas F, Coudert P, Rouvier R, De Rochambeau H. The Rabbit: husbandry, health, and production. Rome: Food and Agriculture organization of the United Nations Rome; 1997.
12. Wan X, Mao L, Li T, Qin L, Pan Y, Li B, Wu X. IL-10 gene polymorphisms and their association with immune traits in four rabbit populations. J Vet Med Sci. 2014;76:369–75.
13. Ren A, Du K, Jia X, Yang R, Wang J, Chen S-Y, Lai S-J. Genetic diversity and population structure of four Chinese rabbit breeds. PLoS ONE. 2019;14:e0222503.
14. Ragab M, Sánchez J, Baselga M. Effective population size and inbreeding depression on litter size in rabbits. A case study. J Anim Breed Genet. 2015;132:68–73.
15. Curik I, Kövér G, Farkas J, Szendrő Z, Romvári R, Sölkner J, Nagy I. Inbreeding depression for kit survival at birth in a rabbit population under long-term selection. Genet Selection Evol. 2020;52:1–13.
16. Broman KW, Weber JL. Long homozygous chromosomal segments in reference families from the centre d'etude du polymorphisme Humain. Am J Hum Genet. 1999;65:1493–500.
17. Kristensen TN, Pedersen KS, Vermeulen CJ, Loeschcke V. Research on inbreeding in the 'omic'era. Trends Ecol Evol. 2010;25:44–52.
18. Kardos M, Luikart G, Allendorf FW. Measuring individual inbreeding in the age of genomics: marker-based measures are better than pedigrees. Heredity. 2015;115:63–72.
19. Peripolli E, Munari D, Silva M, Lima A, Irgang R, Baldi F. Runs of homozygosity: current knowledge and applications in livestock. Anim Genet. 2017;48:255–71.
20. Peripolli E, Munari DP, Silva MVGB, Lima ALF, Irgang R, Baldi F. Runs of homozygosity: current knowledge and applications in livestock. Anim Genet. 2017;48:255–71.

21. Ceballos FC, Joshi PK, Clark DW, Ramsay M, Wilson JF. Runs of homozygosity: windows into population history and trait architecture. Nat Rev Genet. 2018;19:220–34.
22. Kirin M, McQuillan R, Franklin CS, Campbell H, McKeigue PM, Wilson JF. Genomic runs of homozygosity record population history and consanguinity. PLoS ONE. 2010;5:e13996.
23. Pemberton Trevor J, Absher D, Feldman Marcus W, Myers Richard M, Rosenberg Noah A, Li Jun Z. Genomic patterns of homozygosity in worldwide human populations. Am J Hum Genet. 2012;91:275–92.
24. Frankham R, Ralls K. Inbreeding leads to extinction. Nature. 1998;392:441–2.
25. Szpiech ZA, Xu J, Pemberton TJ, Peng W, Zöllner S, Rosenberg NA, Li JZ. Long runs of homozygosity are enriched for deleterious variation. Am J Hum Genet. 2013;93:90–102.
26. Kardos M, Taylor HR, Ellegren H, Luikart G, Allendorf FW. Genomics advances the study of inbreeding depression in the wild. Evol Appl. 2016;9:1205–18.
27. Saura M, Fernández A, Varona L, Fernández AI, de Cara MÁR, Barragán C, Villanueva B. Detecting inbreeding depression for reproductive traits in Iberian pigs using genome-wide data. Genet Selection Evol. 2015;47:1–9.
28. Martikainen K, Sironen A, Uimari P. Estimation of intrachromosomal inbreeding depression on female fertility using runs of homozygosity in Finnish Ayrshire cattle. J Dairy Sci. 2018;101:11097–107.
29. Pacheco HA, Rossoni A, Cecchinato A, Peñagaricano F. Identification of runs of homozygosity associated with male fertility in Italian brown Swiss cattle. Front Genet 2023;14.
30. Bosse M, Megens HJ, Derks MF, de Cara ÁM, Groenen MA. Deleterious alleles in the context of domestication, inbreeding, and selection. Evol Appl. 2019;12:6–17.
31. McQuillan R, Leutenegger A-L, Abdel-Rahman R, Franklin CS, Pericic M, Barac-Lauc L, et al. Runs of homozygosity in European populations. Am J Hum Genet. 2008;83:359–72.
32. Keller MC, Visscher PM, Goddard ME. Quantification of inbreeding due to distant ancestors and its detection using dense single nucleotide polymorphism data. Genetics. 2011;189:237–49.
33. Liu F, Elefante S, Van Duijn C, Aulchenko Y. Ignoring distant genealogic loops leads to false-positives in homozygosity mapping. Ann Hum Genet. 2006;70:965–70.
34. Purcell S, Neale B, Todd-Brown K, Thomas L, Ferreira MAR, Bender D, et al. PLINK: A tool set for Whole-Genome association and Population-Based linkage analyses. Am J Hum Genet. 2007;81:559–75.
35. Howrigan DP, Simonson MA, Keller MC. Detecting autozygosity through runs of homozygosity: a comparison of three autozygosity detection algorithms. BMC Genomics. 2011;12:1–15.
36. Ballan M, Schiavo G, Bovo S, Schiavitto M, Negrini R, Frabetti A, Fornasini D, Fontanesi L. Comparative analysis of genomic inbreeding parameters and runs of homozygosity Islands in several fancy and meat rabbit breeds. Anim Genet. 2022;53:849–62.
37. Schiavo G, Bovo S, Bertolini F, Dall'Olio S, Nanni Costa L, Tinarelli S, Gallo M, Fontanesi L. Runs of homozygosity Islands in Italian cosmopolitan and autochthonous pig breeds identify selection signatures in the Porcine genome. Livest Sci. 2020;240:104219.
38. Brüniche-Olsen A, Kellner KF, Anderson CJ, DeWoody JA. Runs of homozygosity have utility in mammalian conservation and evolutionary studies. Conserv Genet. 2018;19:1295–307.
39. Peripolli E, Stafuzza NB, Munari DP, Lima ALF, Irgang R, Machado MA, et al. Assessment of runs of homozygosity Islands and estimates of genomic inbreeding in Gyr (Bos indicus) dairy cattle. BMC Genomics. 2018;19:34.
40. Zhang Q, Guldbrandtsen B, Bosse M, Lund MS, Sahana G. Runs of homozygosity and distribution of functional variants in the cattle genome. BMC Genomics. 2015;16:542.
41. Liu SQ, Xu YJ, Chen ZT, Li H, Zhang Z, Wang QS, Pan YC. Genome-wide detection of runs of homozygosity and heterozygosity in Tunchang pigs. Animal. 2024;18:101236.
42. Kusza S, Badaoui B, Wanjala G. Insights into the genomic homogeneity of Moroccan Indigenous sheep breeds though the lens of runs of homozygosity. Sci Rep. 2024;14:16515.
43. Li X, Lan F, Chen X, Yan Y, Li G, Wu G, Sun C, Yang N. Runs of homozygosity and selection signature analyses reveal putative genomic regions for artificial selection in layer breeding. BMC Genomics. 2024;25:638.
44. Wang Z, Zhang J, Li H, Li J, Niimi M, Ding G, et al. Hyperlipidemia-associated gene variations and expression patterns revealed by whole-genome and transcriptome sequencing of rabbit models. Sci Rep. 2016;6:26942.
45. Chen S, Zhou Y, Chen Y, Gu J. Fastp: an ultra-fast all-in-one FASTQ preprocessor. Bioinformatics. 2018;34:i884–90.
46. Bai Y, Lin W, Xu J, Song J, Yang D, Chen YE, et al. Improving the genome assembly of rabbits with long-read sequencing. Genomics. 2021;113:3216–23.
47. Li H, Durbin R. Fast and accurate long-read alignment with Burrows–Wheeler transform. Bioinformatics. 2010;26:589–95.
48. Li H, Handsaker B, Wysoker A, Fennell T, Ruan J, Homer N, et al. The sequence alignment/map format and samtools. Bioinformatics. 2009;25:2078–9.
49. Toolkit P. Broad institute, GitHub repository; 2019.
50. McKenna A, Hanna M, Banks E, Sivachenko A, Cibulskis K, Kernytsky A, et al. The genome analysis toolkit: a mapreduce framework for analyzing next-generation DNA sequencing data. Genome Res. 2010;20:1297–303.
51. Chang CC, Chow CC, Tellier LC, Vattikuti S, Purcell SM, Lee JJ. Second-generation PLINK: rising to the challenge of larger and richer datasets. GigaScience 2015;4.
52. Meyermans R, Gorssen W, Buys N, Janssens S. How to study runs of homozygosity using PLINK? A guide for analyzing medium density SNP data in livestock and pet species. BMC Genomics. 2020;21:94.
53. Tao L, Liu H, Adeola AC, Xie H-B, Feng S-T, Zhang Y-P. The effects of runs-of-homozygosity on pig domestication and breeding. BMC Genomics. 2025;26:6.
54. Ferenčaković M, Sölkner J, Curik I. Estimating autozygosity from high-throughput information: effects of SNP density and genotyping errors. Genet Selection Evol. 2013;45:42.
55. Mulim HA, Brito LF, Pinto LFB, Ferraz JBS, Grigoletto L, Silva MR, Pedrosa VB. Characterization of runs of homozygosity, heterozygosity-enriched regions, and population structure in cattle populations selected for different breeding goals. BMC Genomics. 2022;23:209.
56. Wright S. Coefficients of inbreeding and relationship. Am Nat. 1922;56:330–8.
57. Santiago E, Novo I, Pardiñas AF, Saura M, Wang J, Caballero A. Recent demographic history inferred by high-resolution analysis of linkage disequilibrium. Mol Biol Evol. 2020;37:3642–53.
58. Sternstein I, Reissmann M, Maj D, Bieniek J, Brockmann GA. A comprehensive linkage map and QTL map for carcass traits in a cross between giant grey and new Zealand white rabbits. BMC Genet. 2015;16:16.
59. Chesnokov YV, Artemyeva A. Evaluation of the measure of polymorphism information of genetic diversity. Сельскохозяйственная Биология 2015:571–8.
60. Mastrangelo S, Tolone M, Sardina MT, Sottile G, Sutera AM, Di Gerlando R, Portolano B. Genome-wide scan for runs of homozygosity identifies potential candidate genes associated with local adaptation in Valle Del Belice sheep. Genet Selection Evol. 2017;49:84.
61. Quinlan AR, Hall IM. BEDTools: a flexible suite of utilities for comparing genomic features. Bioinformatics. 2010;26:841–2.
62. Huang DW, Sherman BT, Lempicki RA. Systematic and integrative analysis of large gene lists using DAVID bioinformatics resources. Nat Protoc. 2009;4:44–57.
63. Talebi R, Szmatoła T, Mészáros G, Qanbari S. Runs of homozygosity in modern chicken revealed by sequence data. G3 Genes|Genomes|Genetics. 2020;10:4615–23.
64. Wright S. Evolution in Mendelian populations. Genetics. 1931;16:97.
65. Martins TF, Magalhães AFB, Verardo LL, Santos GC, Fernandes AAS, Vieira JIG, Irano N, Dos Santos DB. Functional analysis of litter size and number of teats in pigs: from GWAS to post-GWAS. Theriogenology. 2022;193:157–66.
66. George L, Alex R, Sukhija N, Jaglan K, Vohra V, Kumar R, Verma A. Genetic improvement of economic traits in Murrah Buffalo using significant SNPs from genome-wide association study. Trop Anim Health Prod. 2023;55:199.
67. Shen Q, Martinez G, Liu H, Beurois J, Wu H, Amiri-Yekta A, et al. Bi-allelic truncating variants in CFAP206 cause male infertility in human and mouse. Hum Genet. 2021;140:1367–77.
68. Zhou T-P, Zhang D, Cai L-B, Xu Y-X, Shao L, Liu K-L, et al. Expression of target genes in cumulus cells derived from human oocytes with and without blastocyst formation. Reproductive Dev Med. 2019;3:84–8.
69. Nozawa K, Fujihara Y, Devlin DJ, Deras RE, Kent K, Larina IV, et al. The testis-specific E3 ubiquitin ligase RNF133 is required for fecundity in mice. BMC Biol. 2022;20:161.
70. Do DN, Strathe AB, Ostersen T, Jensen J, Mark T, Kadarmideen HN. Genome-Wide association study reveals genetic architecture of eating behavior in pigs and its implications for humans obesity by comparative mapping. PLoS ONE. 2013;8:e71509.

71. Eckler MJ, McKenna WL, Taghvaei S, McConnell SK, Chen B. Fezf1 and Fezf2 are required for olfactory development and sensory neuron identity. J Comp Neurol. 2011;519:1829–46.
72. Gheyas AA, Vallejo-Trujillo A, Kebede A, Lozano-Jaramillo M, Dessie T, Smith J, Hanotte O. Integrated environmental and genomic analysis reveals the drivers of local adaptation in African Indigenous chickens. Mol Biol Evol. 2021;38:4268–85.
73. Li C, Li J, Wang H, Zhang R, An X, Yuan C, Guo T, Yue Y. Genomic selection for live weight in the 14th month in alpine Merino sheep combining GWAS information. Animals. 2023;13:3516.
74. Yang S, Ning C, Yang C, Li W, Zhang Q, Wang D, Tang H. Identify candidate genes associated with the weight and egg quality traits in Wenshui green Shell-Laying chickens by the copy number Variation-Based Genome-Wide association study. Veterinary Sci. 2024;11:76.
75. Liu Z, Bai C, Shi L, He Y, Hu M, Sun H, et al. Detection of selection signatures in South African mutton Merino sheep using whole-genome sequencing data. Anim Genet. 2022;53:224–9.
76. Liu Y, Li H, Wang M, Zhang X, Yang L, Zhao C, Wu C. Genetic architectures and selection signatures of body height in Chinese Indigenous donkeys revealed by next-generation sequencing. Anim Genet. 2022;53:487–97.
77. Wang Y, Botolin D, Christian B, Busik J, Xu J, Jump DB. Tissue-specific, nutritional, and developmental regulation of rat fatty acid elongases. J Lipid Res. 2005;46:706–15.
78. Crespo-Piazuelo D, Criado-Mesas L, Revilla M, Castelló A, Noguera JL, Fernández AI, Ballester M, Folch JM. Identification of strong candidate genes for backfat and intramuscular fatty acid composition in three crosses based on the Iberian pig. Sci Rep. 2020;10:13962.
79. Corominas J, Ramayo-Caldas Y, Puig-Oliveras A, Pérez-Montarelo D, Noguera JL, Folch JM, Ballester M. Polymorphism in the ELOVL6 gene is associated with a major QTL effect on fatty acid composition in pigs. PLoS ONE. 2013;8:e53687.
80. Wang D, Li X, Zhang P, Cao Y, Zhang K, Qin P, et al. ELOVL gene family plays a virtual role in response to breeding selection and lipid deposition in different tissues in chicken (Gallus gallus). BMC Genomics. 2022;23:705.
81. Zhang Y, Yu M, Dong J, Wu Y, Tian W. Nucleophosmin3 carried by small extracellular vesicles contribute to white adipose tissue Browning. J Nanobiotechnol. 2022;20:165.
82. Chu S, Yang Y, Nazar M, Chen Z, Yang Z. miR-497 regulates LATS1 through the PPARG pathway to participate in fatty acid synthesis in bovine mammary epithelial cells. Genes. 2023;14:1224.
83. Kang K-I, El-Gazzar M, Sellers HS, Dorea F, Williams SM, Kim T, Collett S, Mundt E. Investigation into the aetiology of runting and stunting syndrome in chickens. Avian Pathol. 2012;41:41–50.
84. Hu B, Yang M, Liao Z, Wei H, Zhao C, Li D et al. Mutation of TWNK gene is one of the reasons of runting and stunting syndrome characterized by MtDNA depletion in Sex-Linked Dwarf chicken. Front Cell Dev Biology 2020;8.
85. Mohammadi H, Raffat A, Moradi H, Shoja J, Moradi MH. Estimation of linkage disequilibrium and whole-genome scan for detection of loci under selection associated with body weight in Zandi sheep breed. Agricultural Biotechnol J. 2018;9:151–72.
86. Larson G, Fuller DQ. The evolution of animal domestication. Annu Rev Ecol Evol Syst. 2014;45:115–36.
87. Hewett AM, Stoffel MA, Peters L, Johnston SE, Pemberton JM. Selection, recombination and population history effects on runs of homozygosity (ROH) in wild red deer (Cervus elaphus). Heredity. 2023;130:242–50.
88. Sallam AM, Reyer H, Wimmers K, Bertolini F, Aboul-Naga A, Braz CU, Rabee AE. Genome-wide landscape of runs of homozygosity and differentiation across Egyptian goat breeds. BMC Genomics. 2023;24:573.
89. Consortium IH. A second generation human haplotype map of over 3.1 million SNPs. Nature. 2007;449:851.
90. Kardos M, Åkesson M, Fountain T, Flagstad Ø, Liberg O, Olason P, et al. Genomic consequences of intensive inbreeding in an isolated Wolf population. Nat Ecol Evol. 2018;2:124–31.
91. Zanella R, Peixoto JO, Cardoso FF, Cardoso LL, Biegelmeyer P, Cantão ME, et al. Genetic diversity analysis of two commercial breeds of pigs using genomic and pedigree data. Genet Selection Evol. 2016;48:1–10.
92. McManus C, Facó O, Shiotsuki L, de Paula Rolo JLJ, Peripolli V. Pedigree analysis of Brazilian Morada Nova hair sheep. Small Ruminant Res. 2019;170:37–42.
93. Prieur V, Clarke SM, Brito LF, McEwan JC, Lee MA, Brauning R, Dodds KG, Auvray B. Estimation of linkage disequilibrium and effective population size in new Zealand sheep using three different methods to create genetic maps. BMC Genet. 2017;18:68.
94. Barrett SL, Albertini DF. Cumulus cell contact during oocyte maturation in mice regulates meiotic spindle positioning and enhances developmental competence. J Assist Reprod Genet. 2010;27:29–39.
95. Labrecque R, Sirard M-A. The study of mammalian oocyte competence by transcriptome analysis: progress and challenges. Mol Hum Reprod. 2014;20:103–16.
96. Pokharel K, Peippo J, Weldenegodguad M, Honkatukia M, Li M-H, Kantanen J. Gene expression profiling of corpus luteum reveals important insights about early pregnancy in domestic sheep. BioRxiv. 2020;11:415.
97. Parrilla I, Cambra JM, Cuello C, Rodriguez-Martinez H, Gil MA, Martinez EA. Cryopreservation of highly extended pig spermatozoa remodels its proteome and counteracts polyspermic fertilization in vitro. Andrology. 2024;12:1356–72.
98. Payne F, Colnaghi R, Rocha N, Seth A, Harris J, Carpenter G, et al. Hypomorphism in human NSMCE2 linked to primordial dwarfism and insulin resistance. J Clin Investig. 2014;124:4028–38.
99. Bovo S, Schiavo G, Utzeri VJ, Ribani A, Schiavitto M, Buttazzoni L, Negrini R, Fontanesi L. A genome-wide association study for the number of teats in European rabbits (Oryctolagus cuniculus) identifies several candidate genes affecting this trait. Anim Genet. 2021;52:237–43.

Publisher's note